

## Two-Particle Transfer Reactions: A Key Tool for the Study of Phase Transitions in Nuclei\*

**Andrea Vitturi**<sup>1,2</sup>

<sup>1</sup>Dipartimento di Fisica e Astronomia, Università di Padova, Italy

<sup>2</sup>Istituto Nazionale di Fisica Nucleare, Sezione di Padova, Italy

**Abstract.** In this talk I discuss the possible use of two-particle transfer intensities as a signature of sharp shape transitions. I first consider simple models of phase transitions based on algebraic bosonic approaches, including the case of shape coexistence, showing a dramatic change in the pair-transfer probabilities in correspondence of the critical points. Moving then to a microscopic description of both structure and reaction aspects, I consider as an example the complete series of (t,p) reactions populating the isotope chain of even Zirconium nuclei, to the ground state and to excited  $0^+$  states. One- and two-particle spectroscopic factors derived from Monte Carlo Shell Model calculations are used, together with the sequential description of the two-particle transfer reaction mechanism. The calculation shows a clear signature for a shape phase transition between the spherical  $^{98}\text{Zr}$  and  $^{100}\text{Zr}$ , which displays a coexistence of a deformed ground state with an excited spherical  $0^+$  state. As a result one predicts a weak two-particle cross section from the spherical  $^{98}\text{Zr}$  to the deformed ground state of  $^{100}\text{Zr}$ , with instead a strong population of the spherical excited  $0^+$  state.

The values of the energy of the first  $2^+$  state, the ratio  $E_4/E_2$  and the intensities of the electromagnetic E2 transition connecting ground state and the first excited  $2^+$  state have traditionally been used as order parameters for the shape transitions taking place along a chain of isotopes (or isotones). The discrete control parameter is in these cases given by the number of neutrons (or protons). Two-particle transfer processes, in particular those populating in even-even nuclei the ground state and the other  $0^+$  states, can however provide an additional and complementary clear-cut signature of the occurrence of such phase transitions. In particular one expects at the critical point a sudden weakening of the ground-to-ground pair transition process and a corresponding abnormally strong population of one (or more) excited  $0^+$  states. The characteristic pattern of the pair response should signal not only the occurrence of a shape phase transition, but also the nature of this transition.

The essential quantity that characterizes the system from the pairing point of view is given by the “pairing response”, namely the square of the matrix element of the pair creation (or removal) operator  $P_+ = \sum_j [a_j^\dagger a_j^\dagger]_{00}$  (and similarly for  $P_-$ ), connecting the ground state of a nucleus with  $N$  neutrons with all  $0^+$  states

\*Work done in collaboration with J.A. Lay, L. Fortunato, T. Togashi, Y. Tsunoda and T. Otsuka

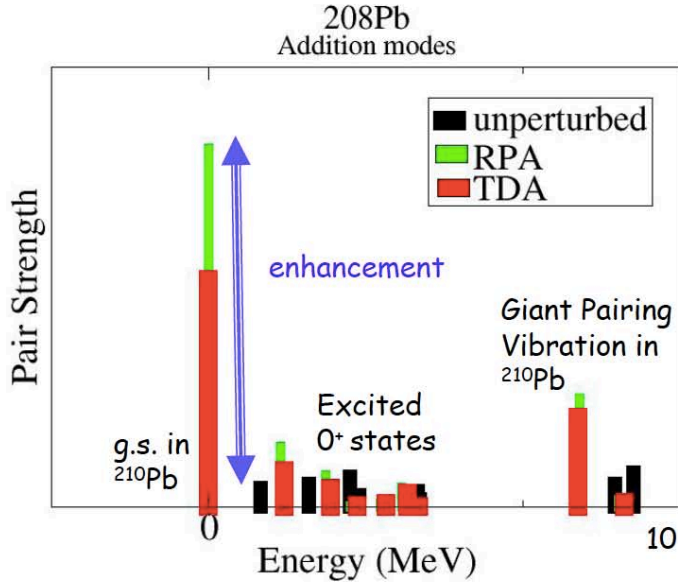


Figure 1. Pairing response in  $^{208}\text{Pb}$  for the neutron pair addition mode, connecting the ground state of  $^{208}\text{Pb}$  with all  $0^+$  states in  $^{210}\text{Pb}$ . The unperturbed response is compared to the one obtained within the particle-particle Tamm-Dancoff and RPA formalism. See Ref. [2].

of nucleus with  $N+2$  (or  $N-2$ ) neutrons (cf. for example Ref. [1]). For simplicity we have considered two-neutron pair operators, but the same arguments would be valid, with proper adjustments, for a proton pair or a proton-neutron  $T = 1$  pair. A typical pairing response is illustrated in Figure 1, referring to the case of pair addition in  $^{208}\text{Pb}$ . The response obtained using particle-particle Tamm-Dancoff or RPA approximation is compared with the unperturbed one. As it is clear from the figure, the inclusion of the residual pairing interaction is strongly enhancing the transition to the ground state, depaupering correspondingly the transition to the excited states. Notice only that the shell gap in the particle-hole states generates the possible occurrence of a second collective state at higher excitation energy (around  $2\hbar\omega$ ), namely the Giant Pairing Vibration.

The pairing response clearly depends on the pairing phase, so a different behavior is expected in the “pairing vibration” regime around closed shells and in the “pairing rotational” regime in the open shell. An example of the ground-to-ground pair strength connecting even Tin isotopes is shown in Figure 2. The calculation, performed within the Hartree-Fock-Bogoliubov model with Skyrme interaction SLy4 and surface-peaked pairing interaction, clearly displays the pairing vibrational behavior around the  $A=100$  and  $A=132$  doubly closed shells and the transition to the superfluid rotational behavior at middle shell. But the pairing response is not only changing when the “pairing phase” changes. A variation

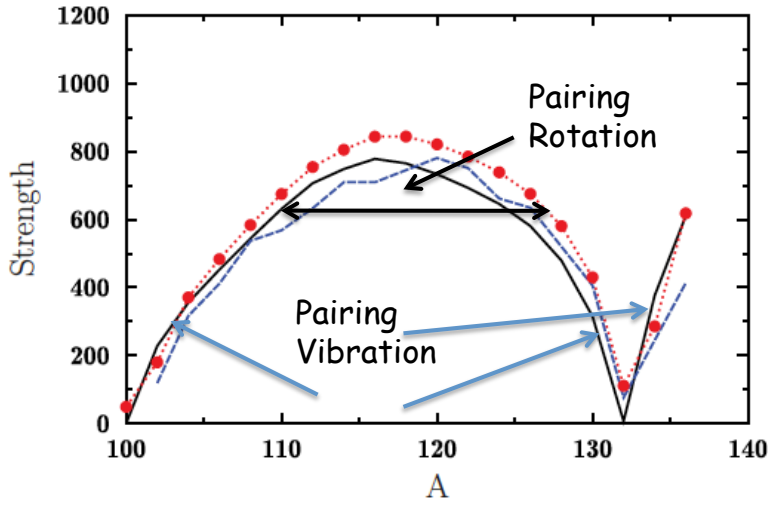


Figure 2. Pair strength connecting the ground states along the chain of even Tin isotopes, obtained in HFB with Skyrme interaction SLy4 and pairing interaction of surface-peaked form. The three calculations refer to different approximation schemes. For details cf. Ref. [3].

of the pair-transfer strength is also expected at the critical points associated to a change of shape of the system along an isotope chain, for example from sphericity to axially-symmetric deformation or to gamma-instability.

To illustrate this point different structure models can be used. A rather simple approach is based on the Interacting Boson Model, by describing series of isotopes in terms of schematic hamiltonians that abruptly performs a transition from  $U(5)$  to either  $O(6)$  or  $SU(3)$ , i.e. from a spherical behavior to the situation of  $\gamma$ -instability or deformed axial symmetry [4,5]. In the example shown in Figure 3 the transition has been assumed to take place at number of boson  $N = 9$ . Within the IBM the pair creation operator, in leading order, is given just by the  $s^\dagger$  operator and one can evaluate the corresponding pair addition intensities obtained by taking the square of the matrix element connecting the ground state in system  $N$  with the ground and excited state in  $N + 1$ . These intensities (for the full response) are shown in Figure 3 for both transitions ( $U(5)$  to  $O(6)$  and  $U(5)$  to  $SU(3)$ ). The figure displays a clear “anomaly” for the pair strength across the change of phase. The pair strength, normally concentrated in the ground-to-ground transition, appears completely fragmented in correspondence of the critical situation, with the ground-to-ground transition that is drastically reduced.

A different physical scenario is that of shape coexistence, where different shape phases occur within the same nucleus and we may face the situation of a (slow or rapid) progressive mixing of spherical and deformed states, eventu-

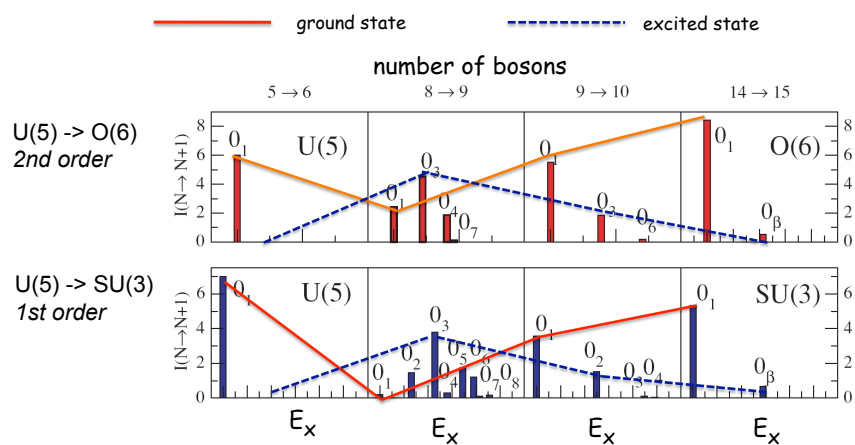


Figure 3. Pairing response for the U(5)-O(6) transition (top row) and the U(5)-SU(3) transition (bottom row). Whereas near the dynamical limits  $U(5)$ ,  $O(6)$  and  $SU(3)$  transfer essentially occurs between ground states (or to lesser degree to the beta-vibrational excited  $0^+$  in the  $SU(3)$  limit), near the critical point  $N = 9$ , the transfer intensity is fragmented over a large number of excited  $0^+$  states. Adapted from Ref. [4].

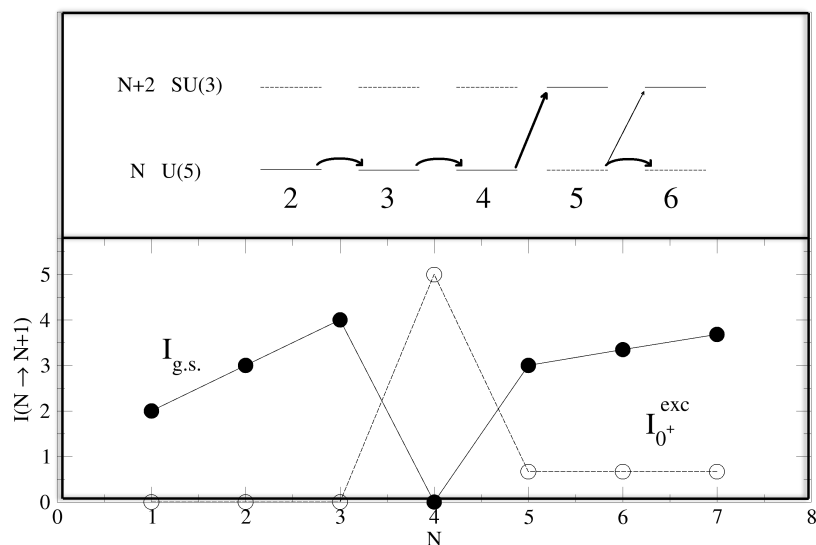


Figure 4. Two-particle transfer intensities to the ground state and to the excited  $0^+$  state in the case of a sequence of isotopes in the presence of shape coexistence. From  $N = 4$  to  $N = 5$  there is the exchange of the spherical ground-state configuration with the “intruder” deformed configuration (cf. text and upper inset).

ally leading to the interchange of the dominant component of these states in the ground state. Again we can have a first guess of the consequences of this situation on the pair-transfer processes within a simplified IBM-like framework. Following the idea of Ref. [6, 7] we can assume for each system characterized by  $N$  valence bosons a possible mixing of a “spherical” state obtained within an IBM  $U(5)$  hamiltonian with another “deformed”  $0^+$  state obtained within a  $SU(3)$  hamiltonian with  $N+2$  bosons, microscopically originated by a 2p-2h core excitation. In this case the pair creation operator will be in leading order given by  $(s^\dagger + s)$ , since we can either add a valence-like boson or destroy the “hole-like” boson. Assuming a sharp transition with increasing number of particles from a fully spherical ground state to a fully deformed ground state (passing from  $N = 4$  to  $N = 5$ , cf. inset in Figure 4), we obtain the pair transfer intensities shown in Figure 4. As in the previous case a clear discontinuity appears at the transition point. However, at variance with the previous case, the pair strength is always practically concentrated in a single state, without the fragmentation illustrated in Figure 3.

We move now from schematic models to a fully microscopic calculation, for both reaction mechanism and structure. We take the case of (t,p) reactions on even-mass Zirconium isotopes, where experimental data at  $E = 20$  MeV are available [8] at least for the lighter systems, i.e. up to  $^{96}\text{Zr}(t,p)$ . Novel interest on Zirconium isotopes has arisen from the recent shell model calculations [9] that indicate in these nuclei a possible case of shape coexistence with a first sharp transition occurring between  $^{98}\text{Zr}$  and  $^{100}\text{Zr}$  (cf. Figure 5). The situation, although much richer, seems therefore to basically resemble the schematic case of shape coexistence displayed in Figure 4.

We have therefore calculated the two-particle transfer probabilities across the phase transition up to  $^{100}\text{Zr}(t,p)$  to the ground and excited  $0^+$  states. In parallel with a detailed microscopic structure description, the reaction process has been also described in microscopic terms. In particular the reaction mechanism has been assumed as the “correlated” sequential single-particle transfer through all intermediate states in the  $A+1$  odd system. Optical models parameters have been taken as in Ref. [8] and single-particle wave functions for the construction of the single-particle form factors have been generated within a Saxon-Woods potential adjusted to yield the proper single-particle energy. This reaction mechanism generates a dynamical dependence on each specific orbit on which the pair is transferred. The transfer probabilities become therefore sensitive not simply to the value of the “global” pair strength, but also to the details of microscopic wave functions [11]. This is better evidenced in Figure 6 where the cross sections associated with single-particle orbits are reported in the case of the  $^{96}\text{Zr}(t,p)^{98}\text{Zr}$  reaction. The collective effects in the pair transfer process comes from the correlations present in both initial and final states that induce a coherent and constructive interference of all the sequential paths (cf. Refs. [1, 10] and references therein). In our case this coherence is obtained by using the two-particle and single-particle spectroscopic amplitudes provided by

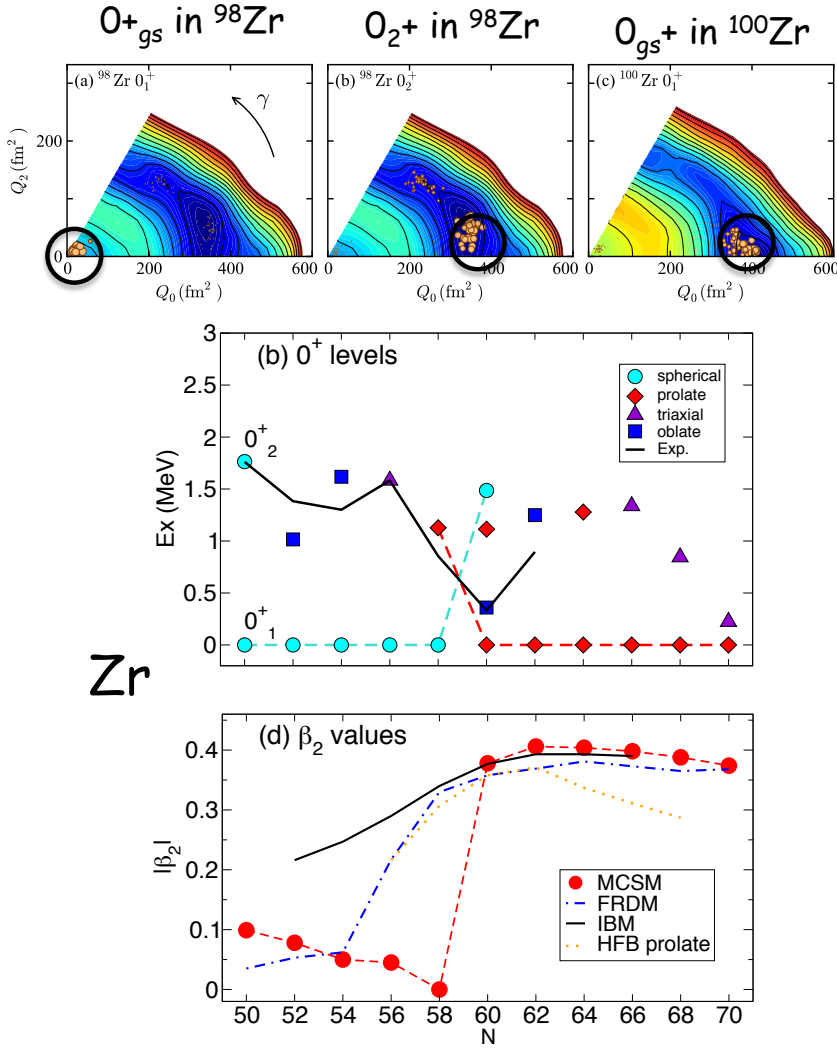


Figure 5. Upper frames: energy surfaces in the  $\beta - \gamma$  plane, showing the change of shape from  $^{98}\text{Zr}$  to  $^{100}\text{Zr}$  (circles indicate the position of the minima). Middle frame: energies of the different  $0^+$  states, with the associated deformations indicated in the inset. Lower frame: ground-state deformation for the different isotopes. Adapted from Ref. [9]

the Monte Carlo Shell Model calculation of Ref. [9]. The largest two-particle amplitudes are reported in Table 1, but also the smaller contributions from the other orbits, included in the model space, have been actually used in the reaction calculation. The constructive effect of the residual pairing-like interaction

## Two-Particle Transfer Reactions

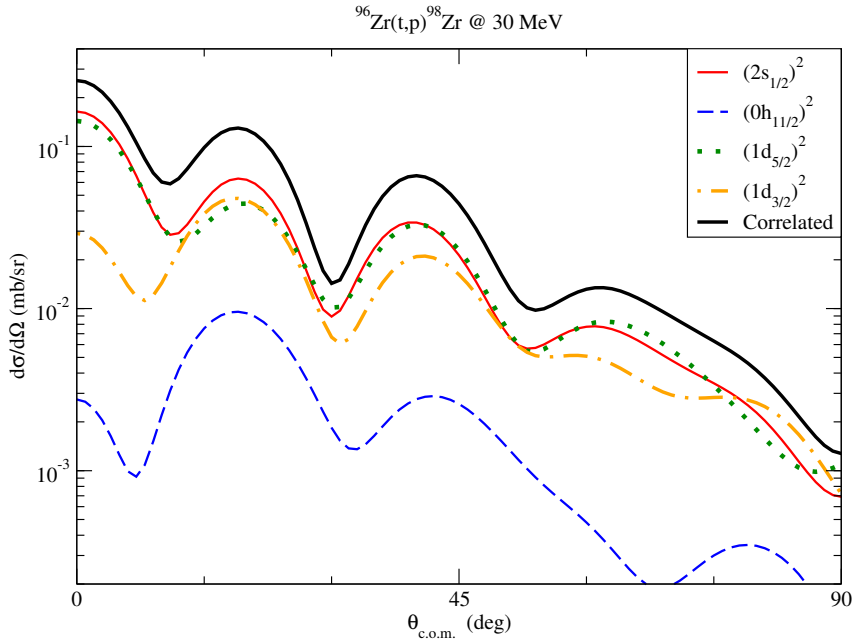


Figure 6. Angular distribution for the reaction  $^{96}\text{Zr}(t,p)^{98}\text{Zr}$  at 30 MeV when the two particles are transferred in a pure single-orbit configuration. The thick solid line gives the result in the case of correlated wave function according to the two-particle amplitudes, the largest being given in Table 1.

is evidenced by the enhancement of the correlated cross section with respect the single particle estimates, as evidenced by Figure 6.

Figure 7 summarizes the results for the full sequence of transfer reactions. The comparison with the experimental data [8] is done by reporting the value of the differential cross section at the first maximum (excluding  $\theta = 0$ ). The overall behavior reproduces the experimental trend, when available. As expected from the amplitudes given in Table 1, in the case of  $^{98}\text{Zr}(t,p)^{100}\text{Zr}$  the

Table 1. Two-particle transfer amplitudes for the different reactions, for the most relevant single-particle orbits. For each case the largest component is bolded.

	90-92	92-94	94-96	96-98	98-100	98-100	100-102
	gs	gs	gs	gs	gs	$0_4^+$	gs
d5/2	<b>0.74</b>	<b>0.86</b>	<b>0.86</b>	0.13	0.0	0.16	0.08
s1/2	0.10	0.08	0.10	<b>0.90</b>	0.0	0.16	0.05
d3/2	0.13	0.18	0.16	0.07	0.0	<b>0.90</b>	0.04
h11/2	0.22	0.20	0.19	0.08	0.0	0.14	<b>0.55</b>

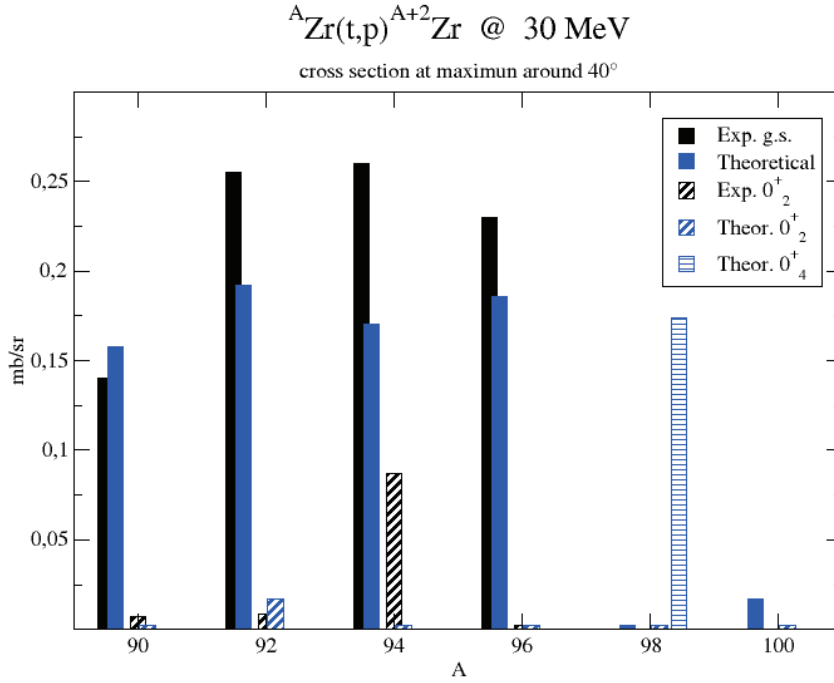


Figure 7. Total integrated cross sections for (t,p) reaction on the different isotopes and specific final states. Experimental values, when available, are also given [8].

calculation predicts a large population of the fourth  $0^+$  state in  ${}^{100}\text{Zr}$ , which displays a “spherical” behavior as the target  ${}^{98}\text{Zr}(\text{gs})$ . Continuing beyond the critical point, we predict again a relatively weak population of the ground state in  ${}^{100}\text{Zr}(t,p){}^{102}\text{Zr}$ , although the reaction connects now two deformed systems with practically the same deformation. In this case this is not due to a structure effect (cfr. the large spectroscopic factors associated with the  $h_{11/2}$  orbit in Table 1) but to the reaction mechanism that does not favor the transfer of a pair in the  $h_{11/2}$  single-particle level.

## References

- [1] R.A. Broglia, O. Hansen, C. Riedel, *Adv. Nucl. Phys.* **6** (1973) 287
- [2] C.H. Dasso, H.M. Sofia and A. Vitturi, *J. Phys.: Conf. Ser.* **580** (2015) 012018
- [3] M. Grasso, D. Lacroix and A. Vitturi, *Phys. Rev. C* **85** (2012) 034317
- [4] R. Fossion, C. E. Alonso, J. M. Arias, L. Fortunato, and A. Vitturi, *Phys. Rev. C* **76** (2007) 014316
- [5] Y. Zhang and F. Iachello, *Phys. Rev. C* **95** (2017) 034306
- [6] P.D. Duval and B.R. Barrett, *Nucl. Phys.* **A376** (1982) 213
- [7] J. E. García-Ramos and K. Heyde, *Phys. Rev. C* **92** (2015) 034309



*Two-Particle Transfer Reactions*

- [8] E.R. Flynn, J.G. Beery and A.G. Blair, Nucl. Phys. **A218** (1974) 285
- [9] Tomoaki Togashi, Yusuke Tsunoda, Takaharu Otsuka, and Noritaka Shimizu, Phys. Rev. Lett. **117** (2016) 172502
- [10] W. Von Oertzen and A. Vitturi, Reports on Progress in Physics **64** (2001) 1247
- [11] J.A.Lay, L.Fortunato and A.Vitturi, Phys. Rev. C **89** (2014) 034618